Wind Energy

WIND ENERGY
Wind Energ. (2015)
Published online in Wiley Online Library (wileyonlinelibrary.com). DOI: 10.1002/we.1855

RESEARCH ARTICLE

A morphing downwind-aligned rotor concept based on a 13-MW wind turbine

Brian Ichter[1], Adam Steele[1], Eric Loth[1], Patrick Moriarty[2] and Michael Selig[3]

[1] Department of Mechanical and Aerospace Engineering, University of Virginia, Charlottesville, VA 22904, USA
[2] National Wind Technology Center, National Renewable Energy Laboratory, Golden, CO 80401, USA
[3] Department of Aerospace Engineering, University of Illinois at Urbana-Champaign, Urbana, IL 61801, USA

ABSTRACT

To alleviate the mass-scaling issues associated with conventional upwind rotors of extreme-scale wind turbines (≥10 MW), a morphing downwind-aligned rotor (MoDaR) concept is proposed herein. The concept employs a downwind rotor with blades whose elements are stiff (no intentional flexibility) but with hub-joints that can be unlocked to allow for moment-free downwind alignment. Aligning the combination of gravitational, centrifugal and thrust forces along the blade path reduces downwind cantilever loads, resulting in primarily tensile loading. For control simplicity, the blade curvature can be fixed with a single morphing degree of freedom using a near-hub joint for coning angle: 22° at rated conditions. The conventional baseline was set as the 13.2-MW Sandia 100-m all glass blade in a three-bladed upwind configuration. To quantify potential mass savings, a downwind load-aligning, two-bladed rotor was designed. Because of the reduced number of blades, the MoDaR concept had a favorable 33% mass reduction. The blade reduction and coning led to a reduction in rated power, but morphing increased energy capture at lower speeds such that both the MoDaR and conventional rotors have the same average power: 5.4 MW. A finite element analysis showed that quasi-steady structural stresses could be reduced, over a range of operating wind speeds and azimuthal angles, despite the increases in loading per blade. However, the concept feasibility requires additional investigation of the mass, cost and complexity of the morphing hinge, the impact of unsteady aeroelastic influence because of turbulence and off-design conditions, along with system-level Levelized Cost of Energy analysis. Copyright © 2015 John Wiley & Sons, Ltd.

KEYWORDS
wind energy; extreme-scale; turbine; morphing; MoDaR

Correspondence
Eric Loth, Department of Mechanical and Aerospace Engineering, University of Virginia, Charlottesville, VA 22904, USA.
E-mail: loth@virginia.edu

Received 20 October 2013; Revised 18 March 2015; Accepted 1 April 2015

1. INTRODUCTION

The average wind turbine rated power has increased 20-fold since 1985, with present large-scale systems greater than 5 MW, as shown in Figure 1.[1] Economies of scale and higher winds aloft are driving systems to ever increasing sizes, and future extreme-scale systems with power levels of 20 MW and have rotor diameters (D) on the order of 240 m. If one assumes that rotor geometry, materials and aeroelastic deflection angles are all held fixed, rotor mass theoretically increases proportional to D^3, i.e. with a scaling exponent of 3. However, continual advances in design and materials have typically allowed smaller exponents. For example, Figure 2 shows the rotor weight scaling for moderate size turbines of 30 m to 120 m in diameter increases with $D^{2.1}$ based on the fit provided by Crawford.[2] Other shave suggested higher exponents for larger turbines, e.g. Rasmussen *et al.*[3] proposed $D^{2.53}$. If one considers recent turbine designs of up to 200 m in diameter,[4] the scaling exponent becomes even greater because of the increased importance of gravity loads, e.g. with increases as large as $D^{3.1}$ as also shown in Figure 2. This scaling is important because the rotor accounts for between 10 and 20% of the initial total system cost, with many other turbine components increasing in scale and cost as the rotor mass increases.[2,5] Furthermore, exponents on the order of 3 suggest that the increase in power will no longer offset the increase in blade mass and cost if even larger diameters are considered. This indicates that new rotor concepts are required to avoid the

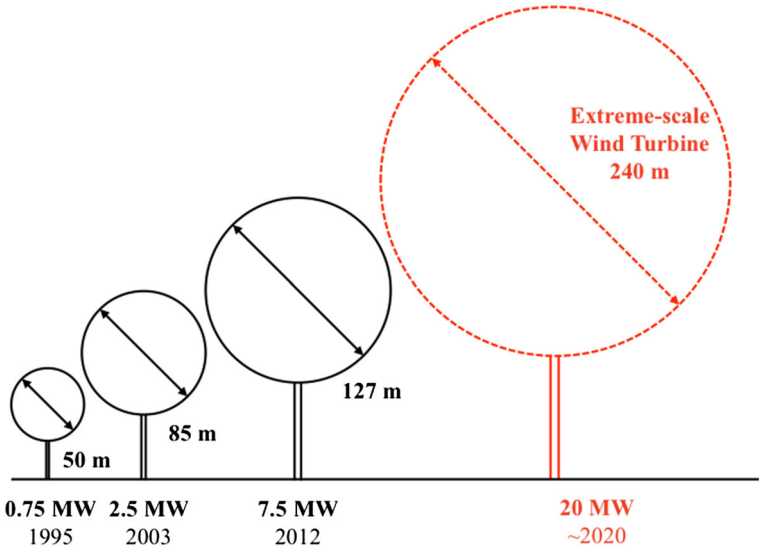

Figure 1. Increase in wind turbine scale and power.[1]

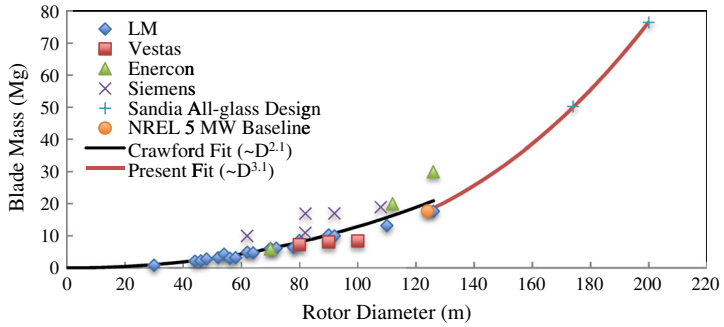

Figure 2. Blade mass vs. rotor diameter showing the scaling relationship with diameter.[2]

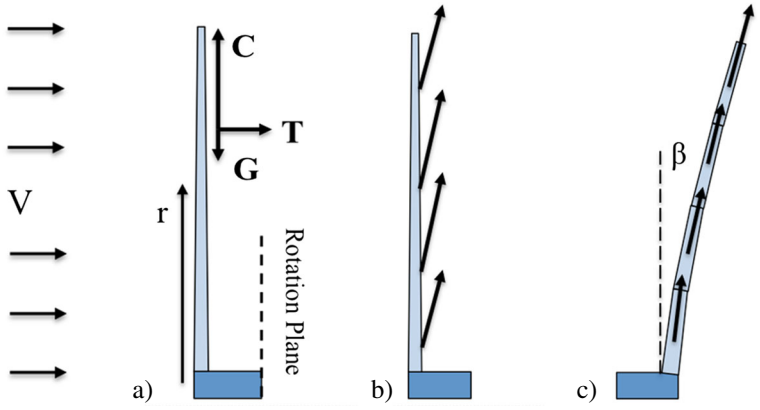

Figure 3. (a) The non-azimuthal forces on a wind turbine blade, (b) the distribution of net force for a conventional upwind rotor blade and (c) the distribution of forces with alignment for a morphing downwind-aligned rotor (MoDaR) blade at rated conditions so downwind cantilever moments are eliminated.

conventional structural constraints associated with extreme scales. As shown in Figure 3(a), (b), these constraints are based on the ability to carry the centrifugal, gravitational and aerodynamic downwind forces. Conventional upwind turbine configurations typically employ blades with fiberglass shells requiring very small aeroelastic deflection to avoid tower strikes

and fatigue. This designed stiffness to avoid tower strikes and fatigue leads to the blade mass problems discussed above. Thus, new concepts in turbine blade design are needed to decrease mass and to address the gravity load barrier.

To relax this conventional stiffness constraint, one may consider adapting the blade geometry to better withstand the imposed loads. Adaptable blade geometry is not a new concept, and it has in fact been used on many successful (and unsuccessful) systems. Downwind coning rotors in particular were proposed by Jamieson and Jaffrey[6] to reduce loads on rotor blades.[6] The downwind soft rotor concept is proposed by Rasmussen *et al.*[3] that allowed the flexible blades to bend downwind and the system to freely yaw to eliminate the need for a mechanical yaw control. A two-bladed 15-kW (13-m diameter) version of this design was field tested where the power and loads were controlled by active stall and coning. Comparison with a similar rigid blade system indicated that rotor loads were reduced by 25–50% during operation as well as in the parked position and in extreme winds. In addition, it was found that aerodynamic efficiency for flexible and downwind-coned rotors was approximately equal to that of rigid rotors of the same disk area. These previous downwind rotor designs by Crawford[2] and Rasmussen *et al.*[3] focused on reducing dynamic loading and fatigue which paved the way for this new concept introduced below. However, the present design focuses on extreme-scale conditions whereby load aligning in the downwind direction is prescribed for certain wind speeds so as to fully minimize rotor mass. For a 5-MW system, these savings are not expected to be significant[7] since the gravity loads are not as intense and since the morphing angles are small (e.g. less than 10° or less). However, as will be shown herein, this downwind-aligning concept can produce significant mass savings (when compared to conventional rotors) for very large systems, e.g. 10 MW or larger.

In this study, a morphing downwind-aligned rotor (MoDaR) concept is put forth to address mass-scaling issues associated with extreme-scale conventional turbines. The concept and its inspiration are introduced in Section 2. Section 3 discusses the structural design and analysis of a conventional upwind rotor compared to the MoDaR concept, which has a 33% reduction in total rotor mass owing to a reduced number of blades. To the authors' knowledge, this is the first study to evaluate an extreme-scale morphing downwind aligned rotor with a previously published conventional upwind rotor. While the simplified present analysis only considers two-dimensional steady-state loads, the results indicate substantial differences between the two rotors in terms of both aerodynamic and structural performance, which should be considered for more detailed investigations.

2. MORPHING ROTOR CHARACTERISTICS

2.1. Concept and bioinspiration

A new extreme-scale concept is introduced which builds off of previous downwind rotor designs (as discussed above and) and uses bio-inspiration (as discussed below) to potentially reduce blade mass. The design proposed herein is termed a morphing downwind-aligned rotor (MoDaR) and is shown in Figure 4(a). The rotor design does not employ a flexible blade, but instead

Figure 4. (a) MoDaR configuration with resultant forces aligned in tension along the blade shown, (b) the shrouded tower, and (c) palm trees bending because of high-speed winds of a hurricane.[9]

the blade is assumed to be stiff with a fixed downwind curvature and a single joint at the hub that can be scheduled over a variety on wind speeds. At the cut-in wind speed, the hub joint at low wind speeds can be locked in the un-morphed configuration so that the rotor has no downwind deflection other than a downwind blade curvature and thus has the maximum energy capture. As the wind speed increases, the rotor can begin to morph to partially align to avoid significant increases in structural stresses then fully align (as in Figure 3(c)) for rated conditions and higher when wind speeds are high enough such that centrifugal forces dominate. Downwind aligning is especially critical for extreme-scale systems, where downwind cantilever forces and gravity stresses rapidly increase blade masses. Because the downwind cantilever loads can be reduced substantially through load alignment, the blades may lend themselves to simplified constructed from joined segments. This segmentation could allow for simplified manufacture, transport and assembly of extreme-scale rotor blades. In the present study, the focus is on the morphing schedule and structural design. The purpose of this analysis is to show the possibility of mass reduction for the morphing downwind-aligned rotor concept. Such mass savings can directly translate into cost savings.[8]

MoDaR employs a downwind design to allow the necessary blade coning angles and because of this, tower wake effects on the rotor play an important role.[10] These tower effects can be addressed by designing a shrouded tower, as shown in Figure 3(b) and detailed in Ref. 11. This aerodynamic fairing resulted in more than a 10-fold reduction in tower drag that correspondingly reduces the wake deficits to be faced by the downwind rotor. The aerodynamic shroud is also self-yawing which can supplement a conventional yaw motor and dynamic yaw stability of a downwind rotor[12] to help minimize yaw error.

This morphing design is bio-inspired, as the benefits of load-alignment can be observed in nature. For example, oak trees have a single section trunk that is stiff and heavy. Under moderate wind conditions, the tree undergoes relatively little deflection, similar to how a conventional turbine blade undergoes little deflection to avoid tower strikes. In high wind conditions, the aerodynamic forces impart extreme cantilever loads on such trees, ultimately destroying them. In contrast, palm trees have a segmented trunk that is able to easily deflect downwind. Under moderate wind conditions, the flexible living structure can bend downwind and alleviate such destructive cantilever aerodynamic loads. In high wind conditions, the flow adaptive nature of the tree allows them to bend all the way to the ground, reducing the total aerodynamic loads (Figure 4). This trunk structure is one of the main reasons why palm trees are much more common near coast lines where hurricane-level winds are common, compared with oak trees or other heavy, stiff trees.

The natural flow adaptability of the palm tree handles aerodynamic loads with minimal structural mass. This bio-inspiration can be similarly used for wind turbines to minimize rotor mass by reducing the conventional stiffness constraint with a downwind blade and reducing stress-inducing non-azimuthal cantilever forces along the blade as shown in Figure 3. In Figure 3 note that the azimuthal (torque-wise) force (F_Q) is needed to generate power, but it is typically an order of magnitude smaller than the other 'non-azimuthal' forces. Figure 3(a) shows the non-azimuthal forces that include centrifugal (C), gravity (G) and thrust forces (T, i.e. downwind aerodynamic force). As wind speed varies, the forces on the blade vary (Figure 5). The changes between cut-in wind speed ($V_{cut\text{-}in}$) and rated wind speed (V_{rated}) arise because the rotor power continually increases; whereas, the changes between rated wind speed and cut-out wind speed ($V_{cut\text{-}out}$) arise because the relative velocity vector of the blade rotates for a fixed power and fixed rotor speed. Based on this variation and an assumed mass distribution (discussed below), the load-path angle along the blade (downwind angle relative to a vertical plane as noted in Figure 3(c)) will vary as a function of wind speed.[8] The forces combine to induce significant cantilever loads in the downwind direction for a conventional blade (Figure 3(b)). As an example, the variation in the rated load alignment angle with rated power can be based on the scaling of Figure 2 for a conventional three-bladed rotor. The results (shown in Figure 6) indicate that the average load-alignment angle increases with rated power. This angle can be compared to the combination of shaft-tilt (5°) and pre-cone (2.5°) used in the NREL 5 MW turbine. The result indicates that the load alignment for turbines of 5 MW or less can be reasonably accommodated with upwind rotors, but that load alignment becomes problematic for upwind turbines of 10 MW or more.

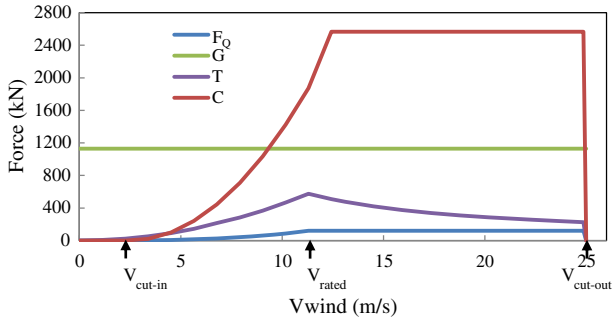

Figure 5. Total forces on a rotor blade as a function of wind speed for a conventional 13.2-MW turbine, where centrifugal forces are generally highest and torque-wise force are smallest.

DOI: 10.1002/we

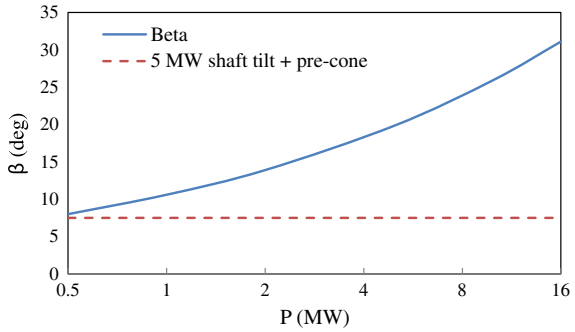

Figure 6. Average load-path angles (over the blade length) at rated conditions as a function of rated turbine power for a two-bladed downwind rotor.

To avoid this problem, a downwind rotor can be used with the rated forces aligned along the blade, which generally results in a curved blade where the tip angle from the vertical is larger than at the hub. In this case, the structural loads act primarily in tension, which greatly reduces stresses for a given structure.[8] The resulting load-path angles (β) that ensure full alignment will vary as a function of radius (R), wind speed (V) and azimuthal angle (ϕ, defined as 0 for vertically upward). In general, full alignment requires that the blade curvature varies with wind speed. However, herein the curvature of the blade is considered fixed while the downwind angle relative to the hub varies with wind speed. This single-joint approach allows for one extra degree of freedom (the morphing angle) per rotor blade, which can simplify control schemes as compared to the multi-jointed approach presented in Ref. 8. By varying this downwind morphing angle, the blade is therefore able to partially or fully align itself to reduce downwind cantilever loads over the entire operating wind range.

2.2. Defining the reference and modar blades

To provide a comparison with the morphing concept for an extreme-scale system, a conventional 13.2-MW turbine configuration was created using aspects of the Sandia 100-m blade and the NREL 5-MW baseline turbine.[4,13] The rated wind speed for both configurations was taken to be 11.3 m/s, which is the same as that provided by Sandia and NREL reference rotors.[4,13] For the conventional rotor, this rated wind speed combined with a tip speed ratio (λ) of 7 yielded a rated tip speed of 80 m/s and a rotational speed of 0.78 rad/s (7.44 rpm). This tip speed ratio approximately coincides with that for a peak power coefficient for a three-bladed turbine as shown by Figure 7 using the WT_Perf computational approach.[14] The cut-in and cut-out speeds, which are based on operational efficiency and safety respectively, were taken as 3 m/s and 25 m/s.[4] To determine the length of the morphing blade, it was decided that the swept area for MoDaR at rated conditions (where the operational morphing angle is largest) would be fixed to be the same as the conventional rotor, i.e. the MoDaR blade swept radius was set at 102.5 m.

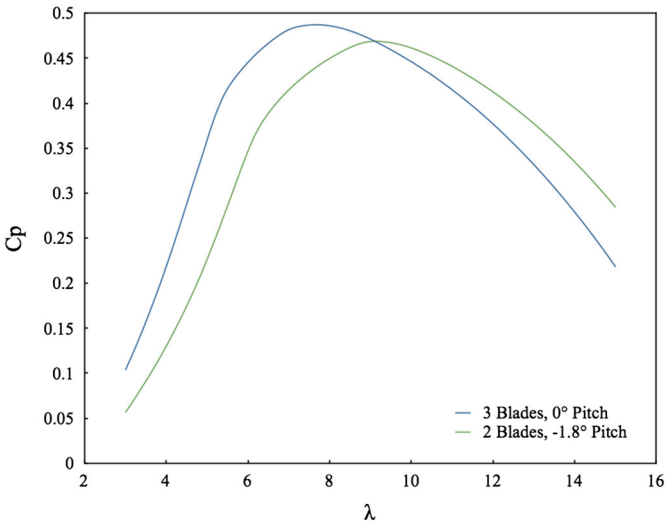

Figure 7. Power coefficient as a function of tip speed ratio for two-bladed and three-bladed systems with optimal pitch angles based on a fixed radius of 102.5 m.

To show how the MoDaR concept can reduce blade mass because of reduced cantilever loads, there are two primary approaches that can be used. The first is to compare a conventional three-bladed upwind rotor to a three-bladed downwind rotor where each downwind blade has lower structural mass, but operates at the same rated tip speed ratio. This approach was previously considered for a 10 MW rotor with an 82 m long blade,[15] and the results indicated that as much as 50% of the blade structural mass can be removed while still limiting the peak stresses for quasi-steady conditions to those seen for a conventional rotor.[15] However, this previous study assumed a relatively high rated wind speed of 14.3 m/s resulting in a low power coefficient and also did not consider the loads for parked conditions.

Herein, a blade-number approach is instead taken to show the potential for rotor mass reduction. In particular, the MoDaR design is assumed to have two downwind blades, where each blade has the same mass and similar design to that of the conventional blades associated with a three-bladed upwind rotor. An advantage of this approach, relative to that used in previously,[15] is that keeping the blade structural characteristics approximately the same allows the parked condition (satisfied with the conventional blades per[4]) to be also implicitly satisfied with the MoDaR blades. Therefore, the challenge of this study is to show that the MoDaR load alignment can accommodate an approximately 50% increase in aerodynamic loads at rated conditions (relative to a conventional blade) without an increase in peak structural stresses (relative to a conventional blade). The present approach also used the reference condition of the 100-m all-glass Sandia blade[4] which beneficially: (i) allows investigation at a higher rated power of 13.2 MW, (ii) allows for the reference conventional blade structure design to be consistent with a well-researched publically available design and (iii) allows for a more typical rated wind speed of 11.3 m/s. However, changing the number of blades changes the optimum top-speed ratio as shown in Figure 7. Here it can be seen that the two-bladed power coefficient curve (optimized in terms of the pitch angle) exhibits a peak at a higher tip speed ratio. Based on these results, a rated tip speed ratio of 8.7 was selected for the two-bladed MoDaR configuration, which corresponds to a tip speed of 98 m/s and a rotational speed 0.96 rad/s (9.17 rpm). Another shortcoming of the two-bladed design is that the peak is at a lower value than for the three-bladed rotor. As a result, the two-bladed downwind blade has a power coefficient of 0.469 (versus 0.487 for a conventional rotor), which represents an overall loss of 3.7% at rated conditions. In addition, a downwind coning angle of 20° will result in a further power loss of 2.5% because of the streamlines being less orthogonal to the rotor plane.[16] As a result, the net power for the MoDAR concept at 11.3 m/s is 12.8 MW, about 6% lower than that for the conventional reference turbine. However, as will be shown later, these morphing aspects of the MoDaR concept will allow it to capture more energy at sub-rated conditions such that the average power captured, once considered over all wind speeds, will be the same as for the conventional rotor.

2.3. Morphing schedule and power capture

For the morphing schedule, the forces were determined based on averaging the net loads for four equal segment lengths assuming a steady wind speed and rotation rate. The net loads were obtained by a steady torque force (F_Q) associated with the aerodynamic power, the gravitational force (G) determined by mass distribution and azimuthal angle, the downwind thrust force (T) determined by two-dimensional lift theory and the centrifugal force (C) determined by mass distribution and angular rotation. The loads are shown in Figure 8 but notably do not include secondary effects of axial induction, so that the results are only first-order approximations.

For a two-bladed rotor, Table I shows the variation in the resulting hub and tip load-path angles at wind speeds between rated and cut-out (which are the highest stress conditions for quasi-steady operation). It can be seen that the load alignment angle generally decreases as the wind speed increases, which is because of the reduced downwind thrust (T). This indicates that blade morphing should take into account the variation in load angle. It can also be seen that the spatial variation in load angle along the blade for a given wind speed is generally small. For example, the average difference between the hub and tip is about 4°. Based on these variations, the morphing concept as a function of wind-speed is shown by the configuration pictures in Figure 9(a)–(d). It employs a single morphing joint near the hub (as shown by arrow in Figure 9(b)) whose angle

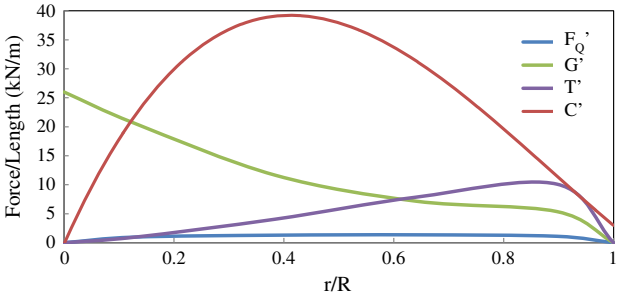

Figure 8. Radial distribution of the forces per unit blade radius at rated conditions for a 13.2-MW conventional blade.

Table I. Downwind load angles at the hub and at the blade tip as a function of wind speed based on a 13.2-MW turbine with two downwind blades. When speed varies, the blade would only be fully aligned if curvature also varied so that both hub and tip both angles were matched. In the present design, the curvature is fixed as 4° and only the hub angle varies.

V/V_{rated}	β_{hub} (°)	β_{tip} (°)	$\beta_{tip} - \beta_{hub}$ (°)
1.00	22.4	27.5	5.1
1.25	17.2	21.0	3.8
1.50	14.0	16.9	2.9
1.75	11.7	14.1	2.4
2.00	10.1	12.0	1.9
2.25	8.8	10.5	1.7

with the vertical is defined as β_{morph} and which varies with the wind speed. Away from this near-hub morphing joint, the blade is assumed to be stiff so the curvature is independent of wind speed.

When the loads are high ($V_{rated} \leq V < 2V_{rated}$), the blade geometry is ideally aligned with the forces (per Figure 3(b)) so that the downwind cantilever loads acting on the blade (and associated stresses) are effectively eliminated. In these 'aligned' conditions, the morphing joint can be set based on the load-angles near the hub, i.e. $\beta_{morph} = \beta_{hub}$. Since, the blade curvature is assumed to be fixed (independent of blade speed), it is not possible to also prescribe the tip angle independently. However, the load-angle variation along the blade, $\beta_{tip} - \beta_{hub}$, did not vary greatly with wind speed (Table I) so the net blade curvature was chosen to be based on $V = 1.25V_{rated}$, which is close to the average value (4°). It should also be noted that such alignment is not critical at sub-rated operational wind speeds ($V_{cut\text{-}in} \leq V < V_{rated}$) because neither structural stresses nor generator power capacity is constraining aspect. Instead, the rotor performance at these lower wind speeds is based on capturing the maximum power possible. To achieve this, the morphing angle was minimized to maximize the capture area and power at these conditions.

The quantitative evolution of the morphing angles with wind speed increases is also shown in the plot of Figure 9. Below the cut-in speed, the rotor is parked, and the blades are held in a vertical plane ($\beta_{morph} = 0$). Above cut-in but below rated conditions, the cantilever forces are generally not large enough to necessitate a full (moment-free) morphing angle. As a

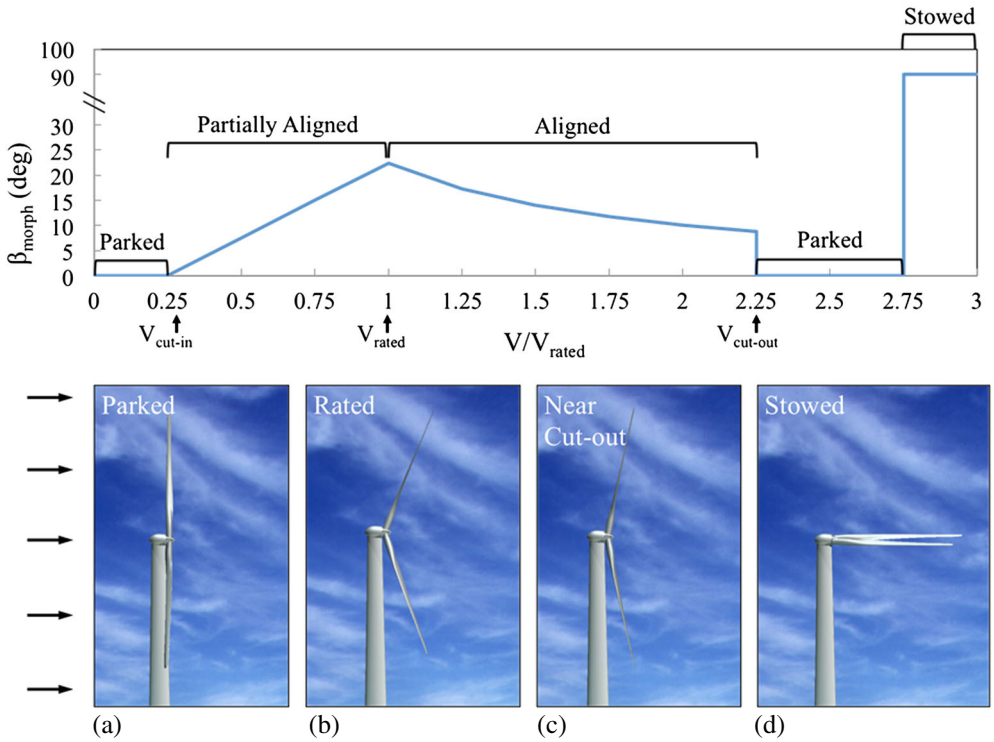

Figure 9. Morphing angle schedule of the MoDaR blade as a function of wind speed (top figure) combined with images of rotor geometry (bottom row) in: (a) parked configuration, (b) aligned at rated speed, (c) aligned just below cut-out speed and (d) stowed for minimum aerodynamic load configuration.

result, the blade morphs from zero alignment to full alignment as the wind speed varies from $V_{cut\text{-}in}$ to V_{rated}, e.g. with a linear increase in downwind angle. For the power-limited condition between V_{rated} and $V_{cut\text{-}out}$, the blade pitches to maintain constant torque and rpm. In this speed range, the MoDaR quasi-steady morphing joint angle is set to be free ($\beta_{morph} = \beta_{hub}$) for optimal load alignment, resulting in a decrease in downwind angle as wind speed increases, from 22.4° at V_{rated} to 8.8° at $V_{cut\text{-}out}$. For wind speeds beyond $V_{cut\text{-}out}$, the rotor generally returns to an upright position, and the blade is parked using collective pitch to feather the blade as is done for a conventional wind turbine. However, if the wind speeds increase further to hurricane-level conditions, the blade may be 'stowed' in a static storage position where $\beta_{morph} = 90°$ to minimize the aerodynamic loads and protect the blades. The morphing schedule associated with Figure 9 can also be seen in the video contained in the Supporting Information.

One concern with stowing blades downwind, as in Figure 9(d), is the increased gravity-based cantilever moment, which may offset some of the benefits associated with the reduced aerodynamic loads. As such, a reduced degree of stowing ($0° < \beta_{morph} < 90°$) may be employed to find the condition that minimizes the combined gravity and aerodynamic loads. Another option with the two-blade design is for one blade to hang vertically downward ($\beta_{morph} = 0°$) in the shadow of the tower while the opposing blade (whose joint points upwards) could be pointed downstream ($\beta_{morph} = 90°$), thereby reducing the net cantilever moment for the rotor by a factor of about two. Yet another option is to avoid the stowing altogether since the MoDaR blades have the same mass and approximate stiffness of the conventional blades, and therefore should be able to withstand the same extreme winds in parked conditions.

To determine the length of the morphing blade, it was decided that the swept area for MoDaR at rated conditions (where the operational morphing angle is largest) should be the same as that for a conventional rotor. Using the fixed 4° blade curvature and the rated (maximum) morphing angle of 22.4°, this resulted with a MoDaR blade length of 110 m, i.e. 10% larger than the conventional rotor blade length. A side benefit of this added length is that the morphed rotor will have a *larger* swept area than the conventional rotor at wind speeds other than rated conditions, as shown in Figure 10(a). Thus more power can be captured both below and above rated conditions. Taking into account only the change in swept area, the increased power output (before rated conditions) and swept area at operating conditions are shown in Figure 10(b). Using a Rayleigh wind speed distribution with an average wind speed of 8.3 m/s, a MoDaR blade captures more energy at the lower speeds. This increased energy capture is counter-balanced by the reductions in the rated power (from 13.2 MW to 12.8 MW) caused by a lower solidity (from having only two blades) and from a reduction in efficiency (from coning). As such both the MoDAR and conventional turbines have the same average output power (5.4 MW) over their operating envelopes. Thus, the concept produces a 33% reduction in rotor mass for the same net energy production.

This rotor mass reduction has some additional benefits, but also some additional problems. For example, the reduced head mass would potentially allow for a reduced tower structure, but the higher rotor frequency for a two-blade design will require a stiffened tower design which serves to generally remove this benefit. Also, the morphed blade tips will be further away from the tower thus potentially reducing tower-strike issues, though the longer blade for the morphing rotor may require a tower height increase of about 8% to maintain ground clearance when $\beta_{morph} = 0$.

3. BLADE STRUCTURAL ANALYSIS

3.1. Blade design and aerodynamic loads for a 10-MW rotor

To analyze the mass saving benefits of a morphing rotor for an extreme-scale wind turbine, a 13.2-MW, three-bladed conventional rotor model (SNL 100-00) and a two-bladed morphing rotor model were created. The mass of individual blades for both rotors was held constant, resulting in a 33% mass reduction for the morphing rotor. In both cases, isotropic materials were combined with quasi-steady on-design stresses to simplify the analysis for this new concept. It should be noted that the present reference blade is relatively heavy (114 200 kg) as compared to the trends shown in Figure 2. For example,

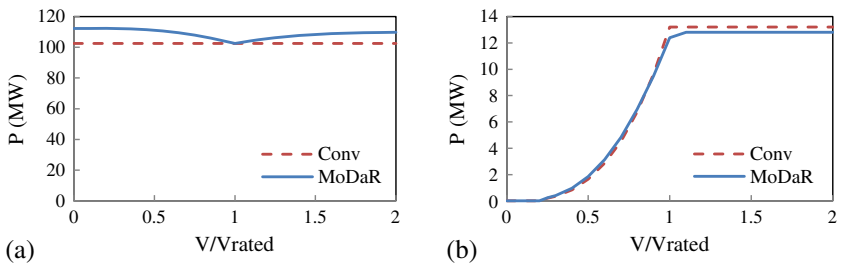

Figure 10. Morphing angle and wind speed effect on (a) swept radius and (b) output power.

the SNL100-002 design additionally uses carbon fiber and core materials that allow for a factor of two reduction in blade mass[17] as is more consistent with the trends of Figure 2. Using this lighter blade would exaggerate the morphing angles results of Section 2.3. However, the present approach with the SNL100-00 as the baseline allows a simpler and more direct comparison since homogeneous material properties can be used. But this first-order approach should only be the first step evaluation of this new concept as more detailed higher-fidelity investigations, e.g. SNL100-002 as the reference, are needed to make a more quantitative assessment of the efficacy of the MoDaR concept.

The airfoil shape, twist and chord distribution along the length of the SNL100-00 13.2-MW blade was geometrically scaled from the National Renewable Energy Laboratory (NREL) offshore 5-MW baseline wind turbine.[4,13] In particular, the connection between the hub and the blade is modeled as a cylinder, which transitions between 15% and 19% of the blade length into a 40.5%-thick, Delft University DU99-W-405 airfoil. From 21% to 65% blade length, the airfoil transitions from the DU99-W-405 to the DU93-W-210. Thereafter, it transitions to the NACA-64-618 for the rest of the blade length. The chord distribution has a maximum chord length at approximately 25% of the blade length. The airfoils were twisted around the quarter chord, assumed to be the pitch axis, and varied from 13.1° at the hub to 0° at the tip. The first-order forces were determined, based on the analysis described in Ref. 8 and mentioned in Section 2.2 for Figure 5, to describe the force per unit radial length distribution along the blade radius as shown in Figure 8.

The internal structure and material were then approximated using the Sandia 100-m all-glass baseline wind turbine blade and NREL 5-MW blade.[4,13] The entire blade (outer shell, spar caps and shear webs) was modeled as a uniform material based on E-LT-5500 fiberglass for simplicity. The modulus of elasticity was specified as 41.8 GPa, the Poisson's ratio as 0.28 and the density as 1920 kg/m^3.[4] Shear webs were located 0.5 m forward and 1.0 m aft of the blade pitch axis for the entire blade length, and a spar cap was placed between them. Shear webs refer to spars that run down the length of the blade, and spar caps refer to a strengthened section of the shell that is between the shear webs as can be seen in Figure 11(a). The purpose of these structures is to increase downwind stiffness and to reduce stress caused by downwind cantilever loads. Since the SNL100-00 included a nearly linear decrease in shell thickness as a function of radial position, the conventional blade design was simplified to have shell thickness that was exactly linearly decreasing from 53 mm at the hub to 13 mm at the tip. The internal structure of the conventional blade can be seen in Figure 11(b). The thickness of the shear webs was prescribed as a constant 9 mm based on the constant thicknesses of the Sandia 100-m blade shear webs.[4] The thickness of the spar cap was chosen as a constant 56 mm. This value was set through a parametric study so as to minimize stress concentrations along the blade.

To find the possible mass reduction allowed by alignment, the morphing rotor used two blades rather than the three blades for the conventional rotor. This allowed for a 33% mass reduction but required that the aerodynamic forces, including torque, be increased by about 50% to have the same power for the rotor. The combination of the increased aerodynamic forces but decreased cantilever moments (because of load alignment) indicated that the morphing blade should have a modified structural design. Based on some optimization for a constant mass blade, the MoDaR shell thickness was more varied, from 68 mm to 8 mm from hub to tip, while shear web thickness was increased (relative to the conventional blade) to 20 m. However, the spar cap thickness of the blade was reduced and was set to vary from 40 mm at the hub to 30 mm at the tip. Finally, to withstand the torque-wise loads when the aerodynamic torque force and the gravitational torque force were aligned, a trailing-edge reinforcement (70 mm thick) and a third shear web (82 mm thick) were added to the trailing edge over the last 5% of the chord length (see Figure 11(c)). This type of additional reinforcement was used in the Sandia 100-m baseline blade[4] and allows for substantially increased ability to withstand torque-wise cantilever forces. These values were determined through parametric optimization to minimize blade stresses at rated conditions.

3.2. Numerical method for structural analysis

To quantify the potential mass savings associated with the morphing aspects, a conventional and a morphing blade model were analyzed using finite element analysis (FEA) with ANSYS (a commercial FEA program). To apply the aerodynamic forces (Figure 8) as a function of radius to the blade, surface elements (SURF154) were overlaid on each mesh element.

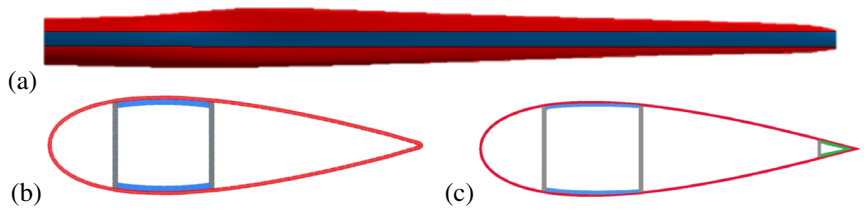

Figure 11. (a) The spar cap (blue) has a constant width based on the Sandia 100-m rotor design, (b) cross section of internal structure for the conventional blade with the spar cap (blue), shear web (grey), shell (red) and (c) the MoDaR blade which also includes a trailing-edge reinforcement (green).[4]

SURF154 have zero thickness and are non-structural; thus, they do not affect the inertial loadings or reinforce the structure of the blade. They are primarily used to apply complex pressure loads. The forces were assigned to each element via an ANSYS command that determined the area of the element and its centroid. Knowing the centroid, the radial location was found and then the pressure was found via a pressure function created from the data in Figure 8. This approach allowed for a near continuous force application as a function of radius. The gravitational and centrifugal forces were applied using the ANSYS built-in inertial loading functionality. A fixed constraint was applied at the hub end of the blade representing the location where the morphing joint is attached to blade. It was assumed that the joint is directly at the interface of the hub and the blade; thus, the entire blade length was simulated. However, additional mass or cost savings may be realized by locating the joint at a more radially outward location.

A computational mesh was created for the blade with maximum element sizes of 0.4 m for the shell and 0.2 m for the shear webs. The shell and shear webs were simulated as separate bodies fixed together. The spar cap was applied by adding a second layer to the shell between the shear webs. The computation was performed with shell elements. In ANSYS, SHELL181 was used, which is a four-node finite strain shell. This shell element is well suited for thin applications. The conventional blade was simulated using an 18 488 element mesh, and the morphing blade was simulated using a 31 332 element mesh.

3.3. Stresses for conventional and morphing blades

Structural Finite Element Analysis (FEA) for a 13.2-MW conventional blade at rated conditions was employed to investigate quasi-steady Von Mises stresses. Both conventional and MoDaR blades were simulated over the range of operating wind speeds and azimuthal angles at all azimuthal angles (φ). As expected, the stresses peaked in the sideways ($\phi = \pi/2$) position, in which gravity acts in the torque-wise direction as shown in Figure 12. The morphing blade was also simulated over the entire range of azimuthal angles and was found to have the same net result. Therefore, the sideways position of $\varphi = \pi/2$ was used to investigate the peak stresses for all wind speeds, e.g. at the rated wind speed shown in Figure 13. For the conventional blade, the maximum stress for the sideways orientation was 79.9 MPa. As can be seen, the peak stresses for the morphing blade (Figure 13(b)) are less than that for a conventional blade (Figure 13(a)) for rated wind speeds, despite a 33% reduction in rotor mass for the former. It is also important to note that the average stresses for the MoDaR design were much lower throughout the blade as compared to the conventional blade.

Using this same approach, the blades were also simulated over the full range of steady operating wind speeds, from no wind to cut-out. The resulting variation in peak stress is shown in Figure 14 for the conventional blade and the MoDaR blade (which uses the morphing schedule of Figure 9). The results indicate that the conventional blade has a peak stress at rated conditions; whereas, the morphing blade peaks at about 1.25 V_{rated} with a stress of 57.3 MPa (28% lower than

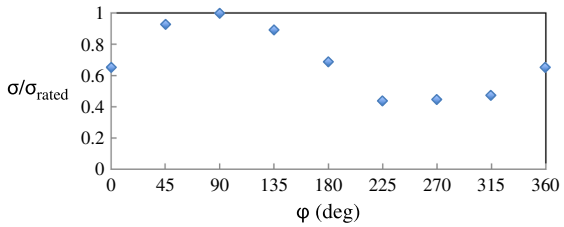

Figure 12. Peak Von Mises stresses at rated wind conditions as a function of azimuthal angle showing that the peak stress occurs at $\varphi = \pi/2$, where the torque and gravitational forces both act downward.[15]

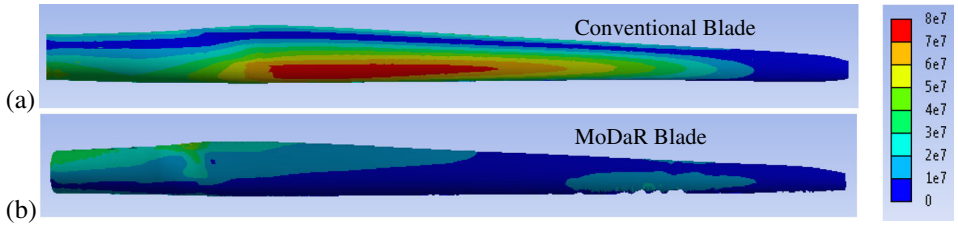

Figure 13. Contour plots of Von Mises stresses (Pa) at the rated condition and $\varphi = \pi/2$ for (a) the conventional blade (for a three-bladed rotor) and (b) the MoDaR blade (for a two-bladed rotor).

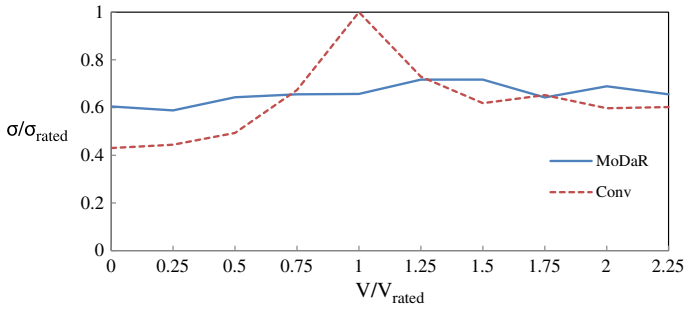

Figure 14. Peak Von Mises stresses of a conventional and MoDaR blade (with curvature optimized for rated conditions) as a function of operating wind speeds. The results show that the conventional rotor overall quasi-steady peak stress (at rated conditions) is always higher than that for the MoDaR design.

the conventional rotor's peak). This peak at non-rated conditions is likely because of the structural design optimization at rated conditions. The morphed-blade stresses are also near constant throughout the operating envelope as the centrifugal and gravity forces tend to dominate. While at some wind conditions the morphing blade stresses exceeded the conventional, the morphing peak never exceeded the peak of the conventional at rated conditions. This indicates that the morphing blade design may be viable when operating in a steady-state wind speed and power-production condition. In addition, because the MoDaR blades have the same mass and material as the conventional blades, they will have similar structural stiffness. As such, they can be expected to have similar resistance to extreme winds in parked conditions, which is important since this was a critical design constraint for the conventional blades.[4]

3.4. Analysis limitations and potential pitfalls for morphing

While the above results indicate significant potential for the morphing downwind-aligned rotor concept for extreme-scale systems (≥10 MW), there are significant limitations associated with the simplified analysis. In particular, the assumption of quasi-steady conditions herein indicates that analysis is needed for unsteady conditions in operating conditions (e.g. to consider flutter and fatigue associated with atmospheric boundary layer turbulence) and for extreme winds (to consider robustness to withstand yawed gusts and hurricane-like conditions). Dynamic analysis is especially needed because two-bladed systems are inherently less stable than three-bladed systems and because of the higher rated tip speed associated with the two-bladed system (22.5% larger).

There are also several challenges associated with the MoDaR concept that could prevent its usage. A challenging case for load-aligned blades is the emergency stop from fully loaded condition, as the blades in this state pitch fast to give negative lift thereby reversing the thrust in which case the load alignment is lost. Another issue that must be considered is that the 22.5% higher rotor frequency for a two-bladed system will necessitate increased tower stiffness to elevate its natural frequency. Fortunately, a 33% saving in rotor mass (if possible) can provide tower stiffening with a 21% increase in natural frequency[18] thereby generally addressing this requirement. The addition of a hinge mechanism may reduce fatigue on the tower and drive train, which could extend the blade lifetime and thus may have a favorable cost impact. However, the morphing mechanism (near-hub joint, actuator and locking mechanism) will add weight and complexity that may negate these savings. In addition, the tower may require increased stiffening to handle the downwind overhang moment for rated conditions (where downwind forces and the morphing angle are high) and to handle two stowed blades pointed downwind if this stowing method is used. Therefore, it is difficult to assess the net cost savings without a full system-level redesign and Levelized Cost of Energy (LCOE) analysis.

The morphing schedule and associated control laws must also be integrated into other control systems that can introduce costly system-level complexity. Furthermore, tower shadow wake effects and potential shroud design[11] will need to be considered in detail to determine impact on blade dynamics particularly when there are rapid changes in wind direction. Finally, all the above differences will need to be considered at a system level in terms of capital and maintenance costs, which will be a difficult analysis considering the viability of the MoDaR concept is at extreme scales. Therefore substantial technical and economic analysis is needed to determine whether the proposed morphing concept will have a positive or negative benefit within cost of energy constraints.

4. CONCLUSIONS

An extreme-scale wind turbine rotor concept was introduced which uses bio-inspiration and builds off of previous downwind rotor designs. The concept was termed a morphing downwind-aligned rotor (MoDaR). This concept allows the blade

forces to be primarily carried in tension by employing curved blades whose joints at the hub can be unlocked to allow for moment-free downwind alignment at wind speeds above rated conditions. The blades can also be scheduled for high swept area capture for wind speed below rated conditions. To investigate whether this load alignment can translate into mass savings, a two-bladed downwind rotor was designed and compared to a conventional three-bladed system, based on the Sandia 100-m all-glass 13.2-MW rotor. For this comparison, both rotors used the same swept radius at rated conditions (102.5 m), same external geometry (scaled from the NREL 5 MW design), same structural material properties and same mass per blade (114 200 kg). This approach allowed blades of similar stiffness and dynamic response such that they can similarly resist extreme winds at parked conditions. By virtue of the reduced number of blades, the two-bladed MoDaR concept had a 33% reduction in total rotor mass but an increase of about 50% in aerodynamic loads.

Based on load alignment, the morphing design yielded a net coning angle of 22.4° at rated conditions (which resulted in a 10% increase in blade length as compared to the conventional non-coned upwind rotor), reducing to 8.8° at cut-out conditions. In addition, a blade downwind curvature of 4° was employed, which was roughly the average required for load alignment between rated and cut-out conditions. In terms of loads supported relative to a conventional rotor, the MoDaR blade had reduced cantilever moments (because of load alignment) that compensated for the increase in aerodynamic forces (because of reduced blade number). This difference in blade loading suggested a modification of the internal dimensions for the MoDaR blades to better optimize the structural performance. In particular, the spar cap thickness was decreased and a trailing edge stiffener was added, all while keeping the blade mass constant. To investigate the relative blade structural performance, a finite element analysis was conducted for the conventional blade as well as the MoDaR blade over all steady-state operating wind speed conditions. The quasi-steady structural analysis indicated that the MoDaR concept had a 28% reduction in the peak structural stress relative to the conventional upwind three-bladed design. In addition, the average stress distribution for the MoDaR blades was reduced even further relative to that of the conventional blade. This substantial stress reduction may make blade segmentation more feasible, which could thereby reduce costs for blade fabrication, transportation, and assembly. However, fully coupled aeroelastic analysis combined with dynamic loading is required to determine whether such mass savings can be realized. In addition, the morphing hinge mass and actuators can also reduce the potential mass savings.

The morphing rotor concept also influenced the power capture. The two-bladed aspect of the MoDaR design required a higher tip speed, which resulted in a lower power coefficient at rated conditions. As a result, the rated power for the MoDaR turbine was reduced to 12.8 MW, and additional losses can occur because of the coning angles. However, the longer blade length for the MoDaR combined with the morphing schedule can increase the captured areas for wind speeds between cut-in and rated conditions. As a result, the average power for the MoDaR was predicted to be 5.4 MW, equal to that of the conventional system. A side benefit of this is that the morphing turbine allows a 3% smaller generator for the same average power produced.

Table II summarizes the potential benefits for the MoDaR concept (relative to the 13.2-MW all-glass Sandia rotor), as well as the key challenges that may prevent its usage. For example, a key benefit is that the MoDaR concept may allow a two-bladed design that could reduce rotor mass and more easily allow blade segmentation. However, the tower may require increased stiffening to handle the downwind overhang moment for rated conditions (where downwind forces and the morphing angle are high) and to handle two stowed blades pointed downwind. Another issue is that developing the morphing mechanism (near-hub joint) and associated control laws may be complex and will require substantial investigation. However, the addition of a hinged mechanism may favorably reduce fatigue on the drive train and other major

Table II. Summary of differences between a conventional rotor and MoDaR.

Aspect	Conventional rotor with Sandia all-glass blades	Morphing downwind-aligned rotor
Swept radius at cut-in	102.5 m	112.5 m
Swept radius at rated	102.5 m	102.5 m
Rated power	13.2 MW	12.8 MW
Average power	5.4 MW	5.4 MW
Capacity factor	0.409	0.422
Number of blades	3	2
Rotor mass	343 Mg	228 Mg
Rotor blade segmentation design	Complex because of high cantilever loads along blade	Potentially eased because of reduced cantilever loads
Hurricane resistance requirements	Requires stiffening for parked rotor blades	Alleviated due to reduced loads using blade stowage
Blade dynamics	Meets requirements	Two-bladed dynamics must be especially addressed
Tower shadow effects	Minimal	Must be addressed
Morphing hinge issues	None	Must be addressed
Tip speed	Conventional (80 m/s)	Higher values (98 m/s) will result in increased noise

structural components which can reduce cost. Thus, the morphing downwind-aligned rotor concept introduced herein may have potential for rotor mass savings but far more analysis (aerodynamic, structural and cost based) is needed to fully evaluate the viability of this concept for extreme-scale turbines. In particular, the effects of turbulence, gust and extreme wind loading, unsteady dynamics and control, impact on fatigue characteristics, acoustic impact and tower shadow will need to be considered in detail to determine whether the proposed concept is practical and economically efficient.

REFERENCES

1. Ashwill TD. Materials and innovations for large blade structures: research opportunities in wind energy technology. *AIAA/ASME/ASCE/AHS*, *ASC Structures*, *Structural Dynamics*, *and Materials Conference*, AIAA Paper 2009–2407, 2009.
2. Crawford C. The path from functional to detailed design of a coning rotor wind turbine concept. *CDEN/C2E2 Conference*, Winnipeg, Manitoba, Canada, 2007.
3. Rasmussen F, Petersen JT, Volund P, Leconte P, Szechenyi E, Westergaard C. *Soft Rotor Design for Flexible Turbines*. Risø National Laboratory: Roskilde, Denmark, Contract JOU3-CT95-0062, 1998.
4. Griffith T, Ashwill TD. *The Sandia 100-meter All-glass Baseline Wind Turbine Blade: SNL100-00*. Sandia National Laboratories: Albuquerque, NM, SAND2011-3779, 2011.
5. Veers P, Ashwill T, Sutherland H, Laird D, Lobitz D, Griffin D, Mandell J, Musial W, Jackson K, Zuteck M, Miravete A, Tsai S, Richmond J. Trends in the design, manufacture and evaluation of wind turbine blades. *Wind Energy* 2003; **6**: 245–259. DOI: 10.1002/we.90.
6. Jamieson P, Jaffrey A. Advanced wind turbine design. *Journal of Solar Energy Engineering* 1997; **119**: 315–320.
7. Ning A, Petsch D. Design optimization of downwind land-based wind turbines. *Wind Energy* 2014.
8. Loth E, Steele A, Ichter B, Selig MS, Moriarty P. Segmented UP-A rotor for extreme-scale wind turbines. *AIAA Aerospace Sciences Meeting*, Nashville, TN, AIAA Paper 2012–1290, 2012.
9. NOAA. Palm tree bending [online]. Available: http://www.photolib.noaa.gov/. (Accessed June 2011)
10. Zahle F, Sorensen N, Johansen J. Wind turbine rotor-tower interaction using an incompressible overset grid method. *Wind Energy* 2009; **12**:594–619. DOI: 10.1002/we.327.
11. O'Connor K, Loth E, Selig M. Design of a 2-D fairing for a wind turbine tower. *31st AIAA Applied Aerodynamics Conference*, San Diego, CA, AIAA Paper 2013–2530, 2013.
12. Thresher R, Dodge D. Trends in the evolution of wind turbine generator configurations and systems. *Wind Energy* 1998; **1**: 70–85. DOI: 10.1002/(SICI)1099-1824(199804).
13. Jonkman J, Butterfield S, Musial W, Scott G. *Definition of a 5-MW Reference Wind Turbine for Offshore System Development*. NREL Technical Publishing: Golden, CO, NREL/TR-500-38060, 2009.
14. Hansen C. AirfoilPrep: an Excel workbook for generating airfoil tables for AeroDyn and WT_Perf [online]. Available: http://wind.nrel.gov/designcodes/preprocessors/airfoilprep/. (Accessed August 2014)
15. Ichter B, Steele A, Loth E, Moriarty P. Structural design and analysis of a segmented ultralight morphing rotor for extreme-scale wind turbines. *AIAA Fluid Dynamics Conference*, New Orleans, LA, AIAA-2012-32170, 2012.
16. Mikkelsen R, Sorensen J, Shen W. Modelling and analysis of the flow field around a coned rotor. *Wind Energy* 2001; **4**: 121–135. DOI: 10.1002/we.50.
17. Griffith D. *The SNL100-02 Blade: Advanced Core Material Design Studies for the Sandia 100-meter Blade*. Sandia National Laboratories: Albuquerque, NM, SAND2013-10162, 2013.
18. Qin C, Loth E. Tower mass savings and energy storage capacity of hydraulic-electric hybrid wind turbines. *2014 Offshore Energy & Storage Symposium*; Windsor, Canada.

SUPPORTING INFORMATION

Additional supporting information may be found in the online version of this article at the publisher's web-site.